 doi:10.20944/preprints202111.0081.v1

Brief Report

What Determines the Parameters of a Propagating Streamer: A Comparison of Outputs of the Streamer Parameter Model and of Hydrodynamic Simulations

Nikolai G. Lehtinen [1]*, Robert Marskar [2]

[1] University of Bergen; nikolai.lehtinen@uib.no
[2] SINTEF Energy Research; Robert.Marskar@sintef.no
* Correspondence: nikolai.lehtinen@uib.no

Abstract: Electric streamer discharges (streamers) in air are a very important stage of lightning, taking place before formation of the leader discharge, and with which an electric discharge starts from conducting objects which enhance the background elecric field, such as airplanes. Despite years of research, it is still not well understood what mechanism determines the values of streamer parameters, such as its radius and propagation velocity. The Streamer Parameter Model (SPM) is aimed to understand this mechanism, as well as to provide a way to efficiently calculate streamer parameters. Previously, we demonstrated that SPM results compared well with a limited set of experimental data. In this Brief Report, we compare SPM predictions to the published hydrodynamic simulation (HDS) results.

Keywords: atmospheric electricity; electric streamer discharges; streamer theory; streamer parameters; plasma instabilities; partially-ionized plasmas

PACS: 52.80.Mg, 92.60.Pw

1. Introduction

Electric streamer discharges, or simply streamers, are ionized columns in gas or liquid which advance by ionizing the material in front of them with the enhanced field at the streamer tip [1,2]. They are an important stage in the formation of sparks, and thus, especially those propagating in air, play a huge role both in technology and natural phenomena such as lightning and Red Sprites. Quantifying streamer properties at high altitudes is important for understanding how lightning interacts with airplanes [e.g., 3,4]. Beside being affected by diverse background conditions, streamer properties may not simply scale in proportion to air density: in particular, the positive streamer threshold field may have nonlinear dependence on air density [5].

Raether [6], Meek [7], and Loeb and Meek [8] were the first to propose that electrons, when undergoing impact ionization avalanche in high electric field in air, create sufficient space charge to form a streamer. In the process of the avalanche-to-streamer transition, electron diffusion plays a crucial role as it determines the transverse size of the avalanche. The same authors also proposed the mechanism of streamer propagation in air, which is based on photoionization. The mechanism works in the following way: (1) UV photons are generated in the streamer head by de-excitation of N_2; (2) photons propagate forward and ionize O_2 in front of the streamer, thereby creating free electrons; (3) the created electrons seed the impact ionization avalanche which propagates in the backward direction in the high field near the streamer tip. This mechanism works for both positive (cathode-directed) and negative (anode-directed) streamers [2, p. 335, 338], however, the difference in electron drift direction makes properties of positive and negative streamers very distinct.

 doi:10.20944/preprints202111.0081.v1

The physics determining the parameters of a propagating streamer discharge in air, such as its radius and speed, had been a long-standing problem [9]. Even though the lateral spreading of an avalanche is due to electron diffusion in the avalanche-to-streamer transition, it may be shown that the diffusion is not the main mechanism due to which the streamer acquires its finite radius [10–12]. In the present work, we calculate corrections to streamer parameters due to electron diffusion and demonstrate that they are insignificant.

The usual approach to theoretical studies of streamers is the numerical solution of the system of coupled electrostatic and hydrodynamic equations for electric field and electron number density. Such hydrodynamic simulations (HDS) are very computationally intensive as they need to have many spatial grid cells in order to resolve well the thin ionization front. This is complicated by the need to resolve other spatial scales, which are very different: the streamer head, which may have a radius of two orders of magnitude larger than the ionization front thickness, and the streamer length, which may be at least an order of magnitude larger than the radius. Despite considerable development effort, HDS still remain challenging as the computational stability and accuracy is achieved only at small grid cell sizes, and therefore, a large number of cells. There exist even more complicated numerical models that attempt to include kinetic effects, such as particle-in-cell (PIC) and hybrid codes. A brief review of the HDS modeling efforts is given in [13].

With the Streamer Parameter Model (SPM), we attempt to uncover the mechanism responsible for the emergence of streamer parameters, and at the same time develop an efficient algorithm for their computation. In Section 3, we demonstrate that SPM results compare reasonably well to those of HDS. This Brief Report applies SPM to positive streamers, however, SPM also makes predictions about negative streamers: in particular, the negative streamer threshold field is calculated to be $E_{-t} \approx 1$ MV/m, which is also observed in experiments [2, p. 362], and, according to the theory of Lehtinen [11,12], is not due to electron attachment process.

2. Streamer Parameter Model (SPM)

The details of the Streamer Parameter Model (SPM) are given in [11,12], and also in an unpublished manuscript [14]. Here, we give a quick overview of the key points of the model.

The streamer under consideration grows with velocity V from a planar electrode, in constant uniform electric field E_e (see Figure 2 in either [11] or [12]). It has a shape of a cylinder (channel), which is attached to the electrode on one end and has a hemispherical cap (head) of the same radius on the other end. The total length of the streamer is L, and the radius of both the head and the channel is a. The electron number density on the axis and electric field inside the streamer are both assumed to be constant and have values of n_s and E_s, respectively. The validity of these assumptions is discussed in Subsection 4.1.

SPM describes a streamer of given length L, in given external field E_e, with the following five unknown parameters: the radius, a, the velocity, V, the field inside the channel, E_s, the electron number density on the axis of the channel, n_s, and the maximum field at the tip, E_m. These parameters are coupled to each other by the following relations:

- **SPM1**: Electrostatic relationship between E_e, E_m, E_s: the field at the streamer tip is enhanced because of available voltage due to difference in E_e and E_s: $\Delta U = (E_e - E_s)L$.
- **SPM2**: Current continuity at the streamer tip: the conductivity current inside the streamer becomes displacement current outside.
- **SPM3**: Ionization/relaxation balance: the maximum ionization time at the streamer tip is approximately equal to the Maxwellian relaxation time inside the streamer.
- **SPM4**: Photo- and impact ionization balance, which provides the relation between V and a.

Preprints (www.preprints.org) | NOT PEER-REVIEWED | Posted: 3 November 2021 doi:10.20944/preprints202111.0081.v1

The algebraic equations corresponding to these relations and the references to the works in which they were originally discussed are given in Lehtinen [11,12].

The system of equations SPM1–SPM4 is sufficient to uniquely determine the set of streamer parameters only if the radius, a, is fixed. This led Lehtinen [11,12] to introduce the notion of 'streamer modes' by analogy with the normal oscillation modes in a linear system. A familiar example of such a system is are infinitesimal perturbations in an unstable uniform plasma, such as a plasma with a uniform electron beam penetrating through it. Let us restrict ourselves to 1D treatment for simplicity. Such a system also possesses one free parameter, namely, the wavelength of a perturbation. Incidentally, this parameter, like a, also has the dimensionality of length. For any given wavelength, the instability growth rate, as well as the proportionality coefficients between amplitudes of perturbations of electric field, electron number density, etc. may be determined. When an unstable linear system develops in time, starting from a random fluctuation with a broad spectrum of wavelengths, only one mode at a single wavelength (the 'preferred' mode), which has the highest growth rate, i.e, is the most unstable, survives in the long run. A less familiar example of an unstable linear system, nevertheless more relevant to the streamer studies, is the planar ionization front and its infinitesimal transverse perturbations. Derks *et al.* [15] have calculated unstable modes and found the preferred mode in this system. The model included electron drift and diffusion, but not photoionization. Unlike these examples, system SPM1–SPM4 is highly nonlinear, and the closest analogy to the growth rate that we can find is the streamer velocity, V. Thus, we propose that the parameters of a physical streamer are described by the system of equations SPM1–SPM4, with a 'preferred' or 'most unstable' radius a at which V is maximized. Selection of the preferred radius by the maximization of velocity may be used in one-dimensional streamer models [16–18] (see also suggestions in Section 4.1 for the future developments of SPM).

Function $V(a)$ is an analog of a 'dispersion function', connecting the temporal and the spatial scale of the system. It is interesting to note that the dependence $V(a)$ indeed has a maximum at a chosen radius, while all other parameters E_s, n_s, E_m have monotonic dependence on a [14]. This peculiar shape of $V(a)$ may be given the following simplified explanation. Velocity is related to the streamer radius by relation SPM4. There exists an approximate version of this relation, first noticed by Loeb [19], which we will now derive. The ionization front thickness (i.e., the avalanche length in the streamer reference frame), d, is related to the radius, a, by $a/d = N_a$, where $N_\mathrm{a} \approx 8$ [10] is number of avalanche lengths required to boost the small number density of photoelectrons ahead of the streamer up to the high electron number density in the channel, n_s. On the other hand, $d \approx V/\nu_t(E_m)$, where $\nu_t(E_m)$ is the net ionization rate, taken at maximum field (see also Subsection 4.2). Thus, velocity V is related to the radius approximately as $V \approx a\nu_t(E_m)/N_\mathrm{a}$. At small radii, even though E_m, and therefore, $\nu_t(E_m)$, is high, proportionality $V \propto a$ dominates and V declines with decreasing a. On the other hand, at large radii a, the field enhancement at the streamer tip (determined by SPM1) becomes smaller. The smaller field yields smaller ionization rate $\nu_t(E_m)$, thus V again declines. We do not exclude the possibility that there exists a gas in which ν_t does not decline fast enough with growing a, and therefore $V(a)$ does not have a maximum. SPM predicts that in such a gas formation of a streamer discharge would be impossible.

3. Results

In our earlier work [11,12], we compared SPM predictions to limited experimental results by Allen and Mikropoulos [20]. Only velocity at streamer length $L = 12$ cm was compared, in a wide range of background fields E_e, with discrepancy not exceeding $\sim 30\%$. In this work, we compare SPM to hydrodynamic simulations (HDS), which were performed by several research groups and presented by Bagheri *et al.* [13]. Such a comparison is grounded in the hypothesis that in HDS, as in nature, the preferred, i.e., the most unstable, mode of the streamer propagation is also being selected.

Preprints (www.preprints.org) | NOT PEER-REVIEWED | Posted: 3 November 2021 doi:10.20944/preprints202111.0081.v1

We consider the same three test cases as Bagheri *et al.* [13] for positive streamers in dry air at 1 bar and 300 K:

1. No photoionization; presence of relatively high background free electron number density of $n_e = 10^{13}$ m^{-3}.
2. No photoionization; presence of relatively low $n_e = 10^9$ m^{-3}.
3. With photoionization and $n_e = 10^9$ m^{-3}. Photoionization is treated with three different approximations to the original description by Zheleznyak *et al.* [21]. These approximations are described in detail in Bagheri *et al.* [13, Appendix A]. In this Brief Report, we label them as 'Luque', 'Bourdon2', and 'Bourdon3', similarly to [13].

Streamer discharges in HDS [13] were simulated between planar electrodes in a square domain with a radius and height of 1.25 cm, with background electric field of $E_e = 1.5$ MV/m. In SPM, however, we only take into account the planar anode, and thus do not reproduce the effects of image charges induced in the cathode or any effects due to the side walls of the simulation domain. In HDS, the positive streamer was started by a small ionized region close to the anode.

Since the background ionization cannot be neglected, it being the only source of free electrons in Cases 1 and 2, in the Appendix we have derived equation (A2), which replaces the photoionization-impact ionization balance equation SPM4. It may include the electron diffusion as a small correction, which is also derived in the Appendix.

For consistency, we used the same functional dependence on electric field E for ionization rate ν_i, attachment rate ν_a, electron mobility μ and electron diffusion coefficient D as Bagheri *et al.* [13]. (In this Brief Report, we often use quantities which are derived from these, namely net ionization rate $\nu_t = \nu_i - \nu_a$ and electron drift velocity $v = \mu E$.) To model photoionization in Case 3, we used the same approximations as Bagheri *et al.* [13] instead of the original Zheleznyak *et al.* [21] expression, which was used in [11,12].

3.1. Case 1

The first test case includes a relatively high background number density of electrons and ions $n_e = 10^{13}$ m^{-3} without photoionization. The results are presented in Figure 1. The black lines reproduce the HDS results presented by Bagheri *et al.* [13]. The maximum field E_m presented in Figure 1b is one of the parameters for which the system SPM1–SPM4 is solved, i.e., one of the immediate outputs of the SPM. The other plots are derived as follows. The streamer length L as a function of time t in Figure 1a is calculated by solving $dL/dt = V(L)$, where $V(L)$ is the output of SPM. The total number of electrons N in Figure 1c was calculated from SPM results as

$$N = \frac{1}{2}\pi a^2 L n_s$$

The factor of $1/2$ is obtained from the consideration that electron number density falls off parabolically towards the walls of the streamer channel, i.e. $n(r) = n_s[1 - (r/a)^2]$. Unfortunately, the HDS results for streamer radius a as a function of L were not available for Case 1 in the form of a plot in [13], but they were available for Cases 2 and 3; we presented SPM calculations of a in Figure 1d anyway.

For sufficiently fine grids good agreement was reached between several HDS codes [13]. We observe that SPM also produces reasonable agreement with HDS, reproducing the same qualitative features:

1. Velocity V in Figure 1a grows with streamer length (and with time).
2. Maximum electric field E_m decreases with streamer length L, at least for the middle values of L (the discrepancies at low and high L are discussed below).
3. Number of electrons grows with L; the rate of growth also increases with L.

In addition to discrepancies caused by approximations in the SPM (see Subsection 4.1), additional discrepancies between the SPM and HDS are caused by the fact that the HDS

Preprints (www.preprints.org) | NOT PEER-REVIEWED | Posted: 3 November 2021 doi:10.20944/preprints202111.0081.v1

simulations did not start at zero L and the field E_m took some time to rise (Figure 1b). Furthermore, at large L, the discrepancy is due to the proximity of the opposite electrode (cathode) in which the image charges are induced that enhance the field in HDS. The cathode, as we already mentioned, was not taken into account in the SPM.

The effect of electron diffusion is included in SPM according to the prescription derived in the Appendix. SPM results with diffusion are shown with dashed lines in Figure 1. We observe that the effect of diffusion is quite small, confirming our estimates in the Appendix and the suggestion of Naidis [10] that it does not affect streamer propagation.

3.2. Case 2

In the second case, the background electron number density is $n_e = 10^9$ m^{-3}. The results are presented in Figure 2, with the same notations as in Figure 1. Lower value of n_e created much steeper gradients in the ionization front, which made HDS computations quite challenging [13]: oscillations in the streamer properties, branching and numerical instabilities were observed. By using a finer grid spacing some groups were able to reach reasonable agreement in their results, without oscillations. Again, SPM produces reasonable agreement with HDS, as in Case 1. The new qualitative feature here, which was not discussed in Case 1, is the growth of radius a with length L, which is present in both HDS and SPM (Figure 2d).

However, SPM in general produced higher fields E_m than HDS, as seen in Figure 2b. This could be due both to errors from approximations made in SPM (see Subsection 4.1) and simulation conditions. The challenges in HDS, caused, e.g., by the fact that higher E_m requires smaller grid step Δx, are discussed in Subsection 4.2. From that discussion, it seems that convergence to the correct solution at $\Delta x \to 0$ was achieved, at least by some of the HDS. The higher field in SPM also led to higher velocity V and smaller radius a, than in HDS.

3.3. Case 3

The third test case includes both small background electron number density $n_e = 10^9$ m^{-3} and photoionization. The photoionization in SPM is implemented in three different approximations, described in Bagheri *et al.* [13, Appendix A] and labeled in Figure 3 as 'Luque', 'Bourdon2', and 'Bourdon3'. The numerical differences in HDS were more significant than the type of approximation [13], and only 'Bourdon3' approximation HDS results are shown in the Figure. The differences in $L(t)$ and $E_m(L)$ due to photoionization approximation choice were presented in Figure 16 of [13]. However, they were too small to draw parallels with analogous differences in SPM.

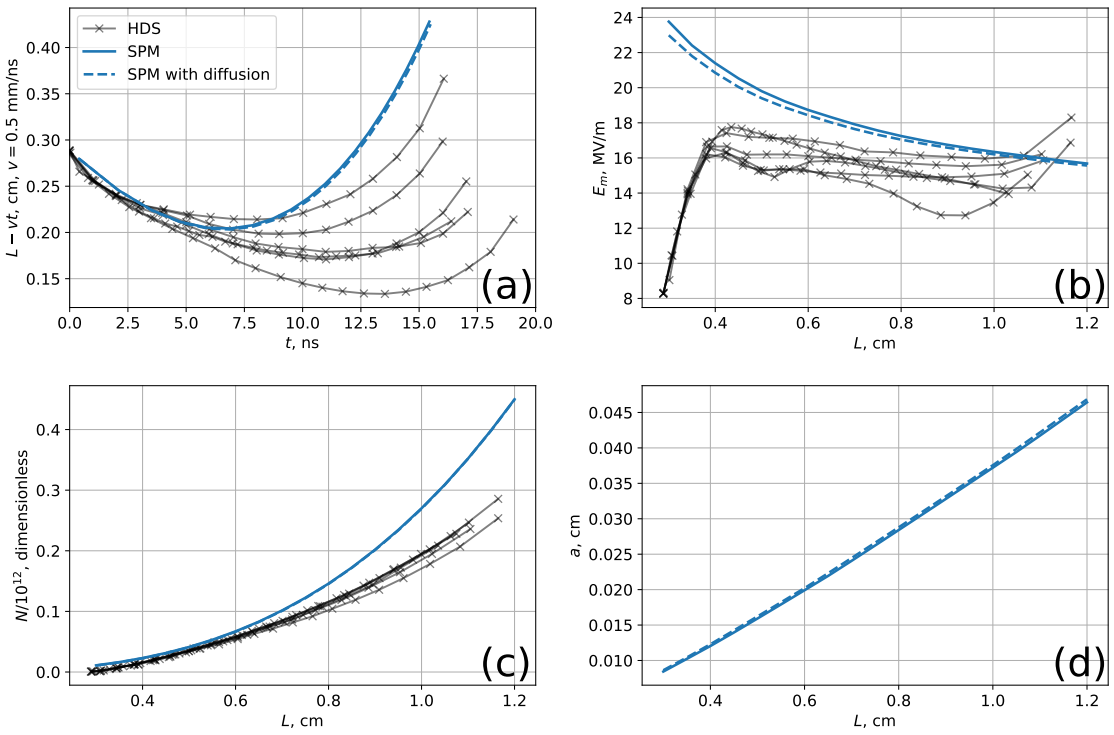

Preprints (www.preprints.org) | NOT PEER-REVIEWED | Posted: 3 November 2021 doi:10.20944/preprints202111.0081.v1

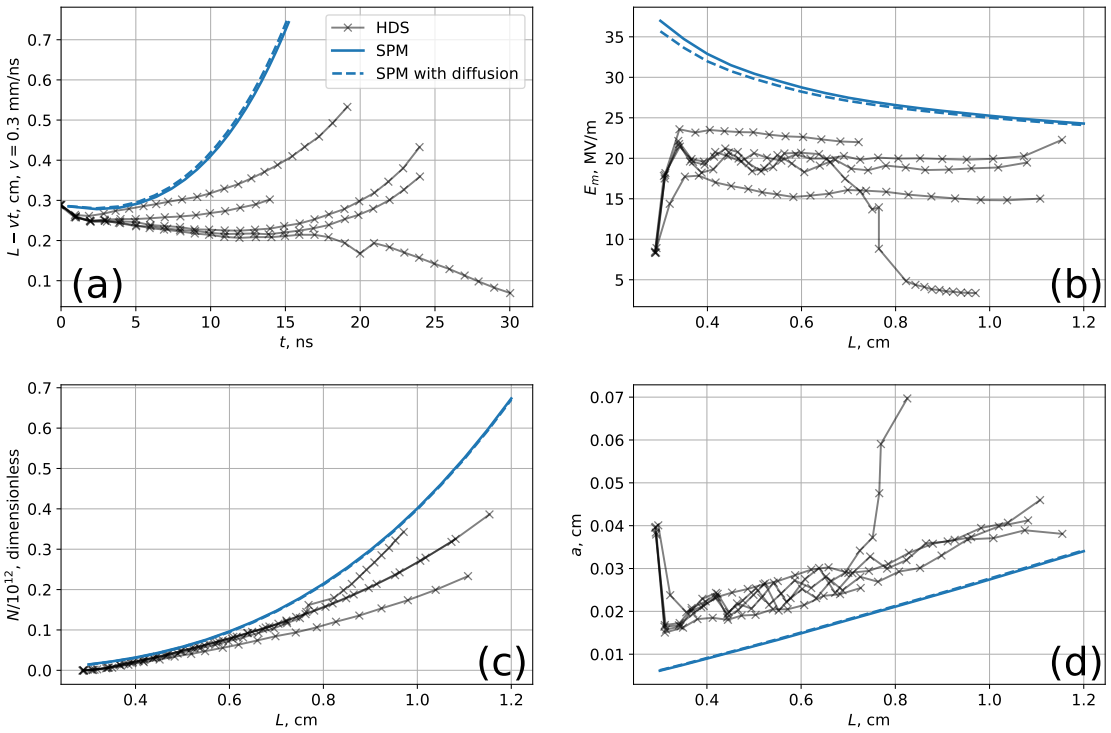

Figure 2. Case 2: Initial background electron number density $n_e = 10^9$ m^{-3}, and no photoionization: (a) length L as a function of time t; (b) maximum electric field E_m as a function of length; (c) total number of produced electrons N as a function of length; (d) streamer radius a as a function of length. Dashed lines denote SPM results with diffusion. Panels (a), (b), (c), (d) correspond to Figures 8, 9a, 9b, 10 in Bagheri *et al.* [13].

Preprints (www.preprints.org) | NOT PEER-REVIEWED | Posted: 3 November 2021 doi:10.20944/preprints202111.0081.v1

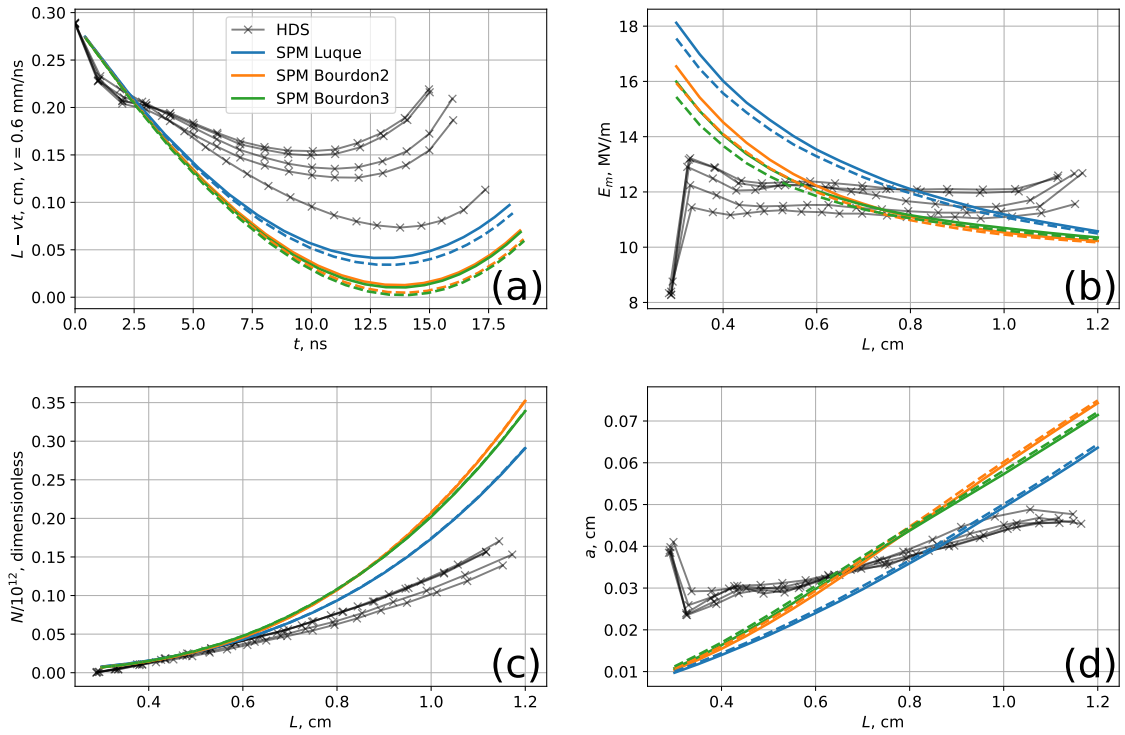

Figure 3. Case 3: Photoionization is present, initial background electron number density is $n_e = 10^9$ m^{-3}: (a) length L as a function of time t; (b) maximum electric field E_m as a function of length; (c) total number of produced electrons N as a function of length; (d) streamer radius a as a function of length. Dashed lines denote SPM results with diffusion. Panels (a), (b), (c), (d) correspond to Figures 13, 14a, 14b, 15 in Bagheri *et al.* [13].

4. Discussion

4.1. Possible errors due to approximations in SPM

Even though SPM, due to absence of any discretization used in HDS, does not have a problem with a steep gradient, there can be significant errors due to approximations made when we reduced a complicated hydrodynamic/electrostatic problem to a small system of algebraic equations SPM1–SPM4. They were discussed in detail in Lehtinen [11,12], so we just briefly mention them here:

1. Radius a enters system SPM1–SPM4 in relations that describe processes at the tip of the streamer. Therefore, value of a is more relevant to the tip curvature radius, than to the radius of the channel, which may be different.
2. We assumed that $n_s = const$ along the axis of the channel. At low external fields E_e, especially those close to the positive streamer threshold $E_{+t} \approx 0.45$ MV/m [2, p. 362], the number of electrons in the channel declines due to attachment. However, for the field $E_e = 1.5$ MV/m used in this work, attachment in the channel can be neglected, especially when using the attachment coefficient expression from Bagheri *et al.* [13] which gives lower values than we would get if the 3-body attachment process were included.
3. Assumption of $E_s = const$ along the channel follows from $n_s = const$ taken together with the assumption of constant current, $J = en_s v(E_s) = const$.

The last assumption deserves more discussion as it may not be valid in some situations. By taking the channel current to be constant along the channel, we assumed that the surface charges on the walls of the channel do not change as the streamer grows, and the new charges are formed only at its head. This assumption seems to be valid for propagating streamers, but breaks down, e.g., for steady-state streamer propagation at E_{+t} [22], in which the charges on the walls of the channel change with time, namely,

Preprints (www.preprints.org) | NOT PEER-REVIEWED | Posted: 3 November 2021 doi:10.20944/preprints202111.0081.v1

drop to zero towards the tail of a finite-length streamer as it moves through the air. In the future versions of SPM, we plan to include E_s and n_s not as single numbers, but as 1D variables that vary along the channel, in order to correctly describe such situations. This will allow to study, e.g., the nature of positive streamer threshold field and positive streamer inception. Understanding and predicting electric field thresholds for streamer inception in diverse conditions inside clouds is going to contribute to understanding airplane-lightning interactions.

4.2. Shortest spatial scale in a streamer and in HDS

The shortest spatial scale in a streamer is found at the streamer front, which has the highest gradient of electron number density and electric field. This scale is given by the thickness of the ionization front, d, and is related (but not equal) to the shortest impact ionization avalanche length, $d_0 = 1/\alpha_t(E_m)$, where α_t is the net ionization coefficient (also called net Townsend coefficient), taken at the maximum field E_m. We may estimate d as [11,12]

$$d = \frac{V \pm v(E_m)}{\nu_t(E_m)} = \left[\frac{V}{v(E_m)} \pm 1\right] d_0,$$

where $\nu_t = v\alpha_t$ is the net ionization rate, $v(E)$ is the electron drift velocity, and upper (lower) sign is for positive (negative) streamers. The elongation ($d > d_0$) in the case of the positive streamer is due to the fact that the backward electron velocity in respect to the moving ionization front is $V + v(E_m)$. Usually the streamer speed is rather high, so that $V \gg v(E_m)$ and $d \gg d_0$. However, under some conditions (examples given below) the streamer speed is low, so it is possible to have $d \approx d_0$. For negative streamers, it is even possible to have $d < d_0$ when V happens to be in the interval $v(E_m) < V < 2v(E_m)$. Incidentally, it is impossible to have $V < v(E_m)$ because then d would be negative. Supposedly, this is the underlying reason for negative streamer threshold of $E_{-t} \approx 1$ MV/m, which was calculated by Lehtinen [11,12].

The ionization front thickness is the shortest spatial scale that has to be resolved in discretized solution methods, such as HDS. The usual criterion for the choice of grid step Δx used in HDS is [13,23–26]:

$$\alpha_t(E)\Delta x = C, \qquad C \lesssim 1, \tag{1}$$

At the streamer front, this is equivalent to $d_0/\Delta x = 1/C$, or

$$\frac{d}{\Delta x} = \frac{V/v(E_m) \pm 1}{C} = N_g$$

i.e., the ionization front thickness is resolved by N_g spatial grid points. For a usual situation $V \gg v(E_m)$, criterion (1) works well even for $C \sim 1$ because even then $N_g \gg 1$. However, for short or narrow streamers, which propagate slowly, velocity V is rather low and may be even lower than the electron drift speed, $v(E_m)$. Below positive streamer threshold E_{+t}, propagating streamers slow down and eventually stop [27]. When such streamers stop propagating, in addition to declining velocity V, we also have shrinking radius $a \to 0$ as well as increasing electric field $E_m \to \infty$, which exacerbates the situation, because d_0 decreases as well. However, in these situations non-local effects [28] also need to be incorporated into the HDS model.

In Case 2 at length $L = 0.35$ cm, the SPM-predicted electric field $E_m \approx 35$ MV/m (see Figure 2b), the velocities are $V \approx 0.3$ mm/ns and $v(E_m) \approx 0.9$ mm/ns, so $d \sim d_0$ and the ionization front is not well resolved when criterion (1) is used with $C \approx 1$ because then $N_g \approx 1$. The situation is improved for a longer (and wider) streamer: when $L = 1$ cm in Case 2, the SPM field $E_m \approx 25$ MV/m, $V \approx 1$ mm/ns and $v(E_m) \approx 0.72$ mm/ns, so $N_g \approx 2.4$ for $C = 1$. The resolution of the ionization front, therefore, is better for a longer streamer with $L = 1$ cm than for a shorter one with $L = 0.35$ cm. Unfortunately,

Preprints (www.preprints.org) | NOT PEER-REVIEWED | Posted: 3 November 2021 doi:10.20944/preprints202111.0081.v1

to get to a longer (and wider) streamer, in this particular case the simulation must first go through the stage with a shorter (and narrower) streamer.

Even though these considerations suggest that the choice of the grid step presented challenges in HDS simulations of Case 2, we do not know the accuracy of the solutions, and thus do not have enough information to state that these challenges were one of the sources of discrepancy. The numerical errors depend also on the choice of the discretization scheme of Poisson and advection-diffusion equations: higher-order methods in both time and space reduce numerical errors, even when N_g is small. Results presented in Figure 11 of Bagheri *et al.* [13] may suggest that the numerical errors in HDS were not large enough to cause the discrepancy between HDS and SPM results for Case 2. In that Figure, it was shown that values of E_m at resolution $\Delta x = 0.8$ μm were only about 5% higher than at $\Delta x = 1.5$ μm. For comparison, at the maximum $E_m \approx 23$ MV/m obtained in HDS, $d_0 \approx 2.7$ μm.

5. Conclusions

We have demonstrated that SPM produces results which are generally in good agreement with HDS, with most discrepancies probably caused by the crudeness of simplifying assumptions in SPM. Some of the discrepancies, however, were due to the different conditions of the problem (streamer starting not from zero length; presence of the opposite electrode). Inclusion of electron diffusion changed the results insignificantly. We suggest that SPM, despite the crudeness of the model, still provides a computationally simple way to reliably assess streamer properties.

Author Contributions: Streamer Parameter Model, writing, discussion, N.L.; writing, discussion, R.M.

Funding: This study was supported by the European Research Council under the European Union's Seventh Framework Programme (FP7/2007-2013)/ERC grant agreement No. 320839 and the Research Council of Norway under contracts 208028/F50, 216872/F50 and 223252/F50 (CoE). R.M. acknowledges funding from the Research Council of Norway grant No. 319930/E20.

Data Availability Statement: The Python3 scripts necessary for running SPM and needed to reproduce the results of this paper are available at https://gitlab.com/nleht/streamer_parameters.

Conflicts of Interest: The authors declare no conflict of interest.

Abbreviations

The following abbreviations are used in this manuscript:

SPM	Streamer Parameter Model
HDS	Hydrodynamic simulation(s)
UV	Ultraviolet
1D	One-dimensional; one dimension

Appendix A

We solve the following continuity equation for electron number density n, in the presence of impact ionization, diffusion and photoionization:

$$-\partial_\xi([V \pm v]n) = \nu_t n + \partial_\xi\left[D\partial_\xi n\right] + s_{\mathrm{ph}}(\xi) \tag{A1}$$

We use the same notations as Lehtinen [11,12]: V is the streamer velocity; $\xi = x - Vt$ is the co-moving coordinate along the streamer axis, with $\xi = 0$ corresponding to the streamer front; ∂_ξ denotes the derivative in respect to ξ; $n(\xi)$ is the electron number density on the axis; v is the electron drift velocity; ν_t is the net ionization rate; $s_{\mathrm{ph}}(\xi)$ is the source of free electrons due to photoionization. The upper (lower) sign is for a positive (negative) streamer. In addition to terms included by Lehtinen [11,12], we

Preprints (www.preprints.org) | NOT PEER-REVIEWED | Posted: 3 November 2021 doi:10.20944/preprints202111.0081.v1

introduced the diffusion term with coefficient D. Values of ν_t, v, D are functions of electric field E, which, in turn, is a function of ξ.

If the diffusion term is neglected, the solution of (A1) is

$$n(\xi) = \frac{1}{V \pm v} \int_{\xi}^{\infty} s_{\mathrm{ph}}(\xi') \exp\left\{ \int_{\xi}^{\xi'} \frac{\nu_t \, d\xi''}{V \pm v} \right\} d\xi' + \frac{C}{V \pm v} \exp\left\{ \int_{\xi}^{\infty} \frac{\nu_t \, d\xi'}{V \pm v} \right\}$$

The integration constant, $C = n_e[V \pm v(E_e)]$, is obtained from the boundary condition $n(\infty) = n_e$, where n_e is the initial background electron number density. By equating $n(0) = n_s$, we get the following condition:

$$\int_0^{\infty} K_{a_{\mathrm{ph}}}(\xi) e^{\gamma(\xi)} \, d\xi + \frac{n_e[V \pm v(E_e)]}{n_s[V \pm v(E_s)]} e^{\gamma(\infty)} = 1, \quad \gamma(\xi) = \int_0^{\xi} \frac{\nu_t \, d\xi'}{V \pm v} \tag{A2}$$

Without photoionization (the first term on the left-hand side) this expression is the same as equation (4) of [10]; without background electrons (the second term) it is the same as SPM4 equation in Section 3.6, item 4 of [11] (Section 4.6, item 4 of [12]). Thus, (A2) should be used instead of SPM4 in the system SPM1–SPM4, when background electron number density $n_e \neq 0$.

Function $K_{a_{\mathrm{ph}}}(\xi)$ is given by

$$K_{a_{\mathrm{ph}}}(\xi) = \frac{s_{\mathrm{ph}}}{n_s[V \pm v(E_s)]} = \int_{r_\perp < a_{\mathrm{ph}}} K(r) \, d^2\mathbf{r}_\perp, \qquad r = \sqrt{\xi^2 + r_\perp^2}$$

and is dependent only on ξ and a_{ph}, which is the effective streamer head radius when it acts as the source of photons (Lehtinen [11,12] assumed $a_{\mathrm{ph}} = a/2$) and $K(r)$ is the kernel of the integral transform which turns $S_i = \nu_i n \approx \nu_t n$ into s_{ph} [21]. In HDS, $K(r)$ is a Helmholtz approximation to the Zheleznyak *et al.* [21] model [13, Appendix A].

Let us now tackle the correction due to diffusion and demonstrate that it is small. From now on, we neglect the photoionization term in (A1), since the diffusion is important only in the region where n is already high and the impact ionization term dominates as the source of free electrons. Substitute

$$\partial_\xi n = -\frac{\nu_t \pm \partial_\xi v}{V \pm v} n$$

into the diffusion term in (A1) and transfer it to the left-hand side:

$$-\partial_\xi \left(\left[V \pm v - D \frac{\nu_t \pm \partial_\xi v}{V \pm v} \right] n \right) = \nu_t n$$

This looks like (A1) without diffusion, with substitution

$$V \pm v \longrightarrow (V \pm v) \left(1 - \frac{D(\nu_t \pm \partial_\xi v)}{(V \pm v)^2} \right)$$

which we can also make in formula (A2) to get condition SPM4 in the next order of approximation. For $V \gtrsim 0.3$ Mm/s, $\nu_t \lesssim 10^{11}$ s^{-1} (which is valid for $E \lesssim 15$ MV/m), $D \approx 0.1$ m^2/s and with estimated values of $|\partial_\xi v| \lesssim v/a$ for $a \gtrsim 0.1$ mm, the correction multiplication factor is different from unity by no more than 10%, which justifies this perturbation approach.

References

1. Bazelyan, E.M.; Raizer, Y.P. *Spark Discharge*; CRC Press: New York, 1998.
2. Raizer, Y.P. *Gas discharge physics*; Berlin: Springer, 1991.
3. van Deursen, A.; Kochkin, P.; de Boer, A.; Bardet, M.; Allasia, C.; Boissin, J.F.; Flourens, F. Lightning current distribution and hard radiation in aircraft, measured in-flight. 2017 International Symposium on Electromagnetic Compatibility - EMC EUROPE, 2017, pp. 1–4. doi:10.1109/EMCEurope.2017.8094765.

4. Skeie, C.A.; Østgaard, N.; Lehtinen, N.G.; Sarria, D.; Kochkin, P.; de Boer, A.I.; Bardet, M.; Allasia, C.; Flourens, F. Constraints on Recoil Leader Properties Estimated from X-ray Emissions in Aircraft-Triggered Discharges. *J. Geophys. Res. Atmos.* **2020**, *125*, e2019JD032151. doi:10.1029/2019JD032151.
5. Phelps, C.T.; Griffiths, R.F. Dependence of positive corona streamer propagation on air pressure and water vapor content. *Journal of Applied Physics* **1976**, *47*, 2929–2934. doi:10.1063/1.323084.
6. Raether, H. Die Entwicklung der Elektronenlawine in den Funkenkanal. *Z. Physik* **1939**, *112*, 464–489. doi:10.1007/BF01340229.
7. Meek, J.M. A Theory of Spark Discharge. *Phys. Rev.* **1940**, *57*, 722–728. doi:10.1103/PhysRev.57.722.
8. Loeb, L.B.; Meek, J.M. *The Mechanism of the Electric Spark*; Stanford University Press: Stanford University, California, 1941.
9. Ebert, U.; Sentman, D.D. Streamers, sprites, leaders, lightning: from micro- to macroscales. *J. Phys. D: Appl. Phys.* **2008**, *41*, 230301.
10. Naidis, G.V. Positive and negative streamers in air: Velocity-diameter relation. *Phys. Rev. E* **2009**, *79*. doi:10.1103/PhysRevE.79.057401.
11. Lehtinen, N.G. Physics and mathematics of electric streamers. *Izv. VUZov (Radiofizika)* **2021**, *64*, 12–28. in Russian, doi:10.52452/00213462_2021_64_01_12.
12. Lehtinen, N.G. Physics and mathematics of electric streamers. *Radiophysics and Quantum Electronics* **2021**. in print.
13. Bagheri, B.; Teunissen, J.; Ebert, U.; Becker, M.M.; Chen, S.; Ducasse, O.; Eichwald, O.; Loffhagen, D.; Luque, A.; Mihailova, D.; Plewa, J.M.; van Dijk, J.; Yousfi, M. Comparison of six simulation codes for positive streamers in air. *Plasma Sources Science and Technology* **2018**, *27*, 095002. doi:10.1088/1361-6595/aad768.
14. Lehtinen, N.G. Electric streamers as a nonlinear instability: the model details, 2020. arXiv:2003.09450 [physics.plasm-ph].
15. Derks, G.; Ebert, U.; Meulenbroek, B. Laplacian Instability of Planar Streamer Ionization Fronts—An Example of Pulled Front Analysis. *Journal of Nonlinear Science* **2008**, *18*, 551. doi:10.1007/s00332-008-9023-0.
16. Aleksandrov, N.L.; Bazelyan, E.M. Temperature and density effects on the properties of a long positive streamer in air. *Journal of Physics D: Applied Physics* **1996**, *29*, 2873–2880. doi:10.1088/0022-3727/29/11/021.
17. Guo, J.M.; Wu, C.H. Streamer radius model and its assessment using two-dimensional models. *IEEE Transactions on Plasma Science* **1996**, *24*, 1348–1358. doi:10.1109/27.553200.
18. Pavan, C.; Martinez-Sanchez, M.; Guerra-Garcia, C. Investigations of positive streamers as quasi-steady structures using reduced order models. *Plasma Sources Sci. Technol.* **2020**, *29*, 095004. doi:10.1088/1361-6595/aba863.
19. Loeb, L.B. Ionizing Waves of Potential Gradient. *Science* **1965**, *148*, 1417–1426. doi:10.1126/science.148.3676.1417.
20. Allen, N.L.; Mikropoulos, P.N. Dynamics of streamer propagation in air. *J. Phys. D: Appl. Phys.* **1999**, *32*, 913. doi:10.1088/0022-3727/32/8/012.
21. Zheleznyak, M.B.; Mnatsakanyan, A.K.; Sizykh, S.V. Photo-ionization of nitrogen and oxygen mixtures by radiation from a gas-discharge. *High Temp. (USSR)* **1982**, *20*, 357–362.
22. Francisco, H.; Bagheri, B.; Ebert, U. Electrically isolated streamer heads formed by strong electron attachment. *Plasma Sources Sci. Technol.* **2021**, *30*, 025006. doi:10.1088/1361-6595/abdaa3.
23. Villa, A.; Barbieri, L.; Gondola, M.; Leon-Garzon, A.R.; Malgesini, R. Mesh dependent stability of discretization of the streamer equations for very high electric fields. *Computers & Fluids* **2014**, *105*, 1–7. doi:10.1016/j.compfluid.2014.09.002.
24. Teunissen, J.; Ebert, U. Simulating streamer discharges in 3D with the parallel adaptive Afivo framework. *J. Phys. D: Appl. Phys.* **2017**, *50*. doi:10.1088/1361-6463/aa8faf.
25. Marskar, R. An adaptive Cartesian embedded boundary approach for fluid simulations of two- and three-dimensional low temperature plasma filaments in complex geometries. *J. Comput. Phys.* **2019**, *388*, 624–654. doi:10.1016/j.jcp.2019.03.036.
26. Marskar, R. 3D fluid modeling of positive streamer discharges in air with stochastic photoionization. *Plasma Sources Sci. Technol.* **2020**, *29*, 055007. doi:10.1088/1361-6595/ab87b6.
27. Pancheshnyi, S.V.; Starikovskii, A.Y. Stagnation dynamics of a cathode-directed streamer discharge in air. *Plasma Sources Sci. Technol.* **2004**, *13*, B1. doi:10.1088/0963-0252/13/3/B01.
28. Naidis, G.V. Effects of nonlocality on the dynamics of streamers in positive corona discharges. *Technical Physics Letters* **1997**, *23*, 493–494. doi:10.1134/1.1261717.